International Institute of Welding
A world of joining experience

IIW- X-1668-09 , IIW-XIII-2291-09, IIW-XV-1326-09

Report on the Round Robin Tests on Residual Stresses 2009
Joint Working Group of Commission X/XIII/XV

New calculations checking an adequate materials law,
New results on distortion measurements

Coordinator Helmut Wohlfahrt [1],
in cooperation with Jens Sakkiettibutra[2] and Tobias Loose[3] (new calculations),
Markus Brand [4] (distortion measurements), Dieter Siegele[4] and
Thomas Nitschke-Pagel[1] (discussions), Thomas Nitschke-Pagel [1] (reporter)

[1]Institut für Füge- und Schweißtechnik, University of Braunschweig, [2] Bremer Institut für angewandte Strahltechnik GmbH, Bremen, [3] Ingenieurbüro Tobias Loose GbR, Karlsruhe, [4] Fraunhofer-Institut für Werkstoffmechanik

1. Introduction

Table 1 offers final information about all institutions participating in the programme of residual stress measurements. It is a fact that all measurements revealed a relative minimum of the longitudinal residual stresses at the centre line of the weld seam and maxima in distances between 5 and 8 mm from the centre line. These maxima are really pronounced (up to 500 MPa) and have been found in surface layers as well as in a depth below surface of 3 mm. Measurements of the transverse residual stresses indicate a deep minimum in the compressive range at the weld centre line mainly in a very thin surface layer (measurements by means of X-rays) and the maximum stress values in some distance from the centre line are not as big as the longitudinal stress maxima.

The calculations reported in [1, 2] reveal neither a minimum of the longitudinal residual stresses at the weld centre line nor a maximum in a distance between 5 mm and 8 mm from the weld centre line (Fig. 1). Concerning the transverse residual stresses the calculations show a minimum at the weld centre line with magnitudes between -50 MPa and +50 MPa and tensile maxima in a bigger distance from the centre line and with lower magnitudes than measured by means of X-rays. Fig. 1 and Fig. 2 present comparisons of calculated and measured residual stresses [1, 2]. Additionally Fig. 3 and Fig.4 indicate once more examples of the significance of the maxima in the distributions of longitudinal residual stress measured with different techniques.

Some papers in literature offered the advice to check whether the kinematic hardening model used by the cited calculations is really adequate for the residual stress evaluation in a welded austenitic steel plate. Kinematic hardening takes into account the Bauschinger effect really strictly. The

---

[1] J.J. Janosch: Round robin phase II – 3D modelling, Updated results. IIW-X/XIII/XV-RSDP-114-05
[2] Jean-Jacques Janosch: International Institute of Welding work on residual stress and its application to industry. International Journal of Pressure Vessel and Piping 85 (2008) 183-190

Table 1 Presentation of the institutions participating in the IIW Round Robin "Residual Stress Measurements" and scheme for the distribution of the three welded austenitic steel plates

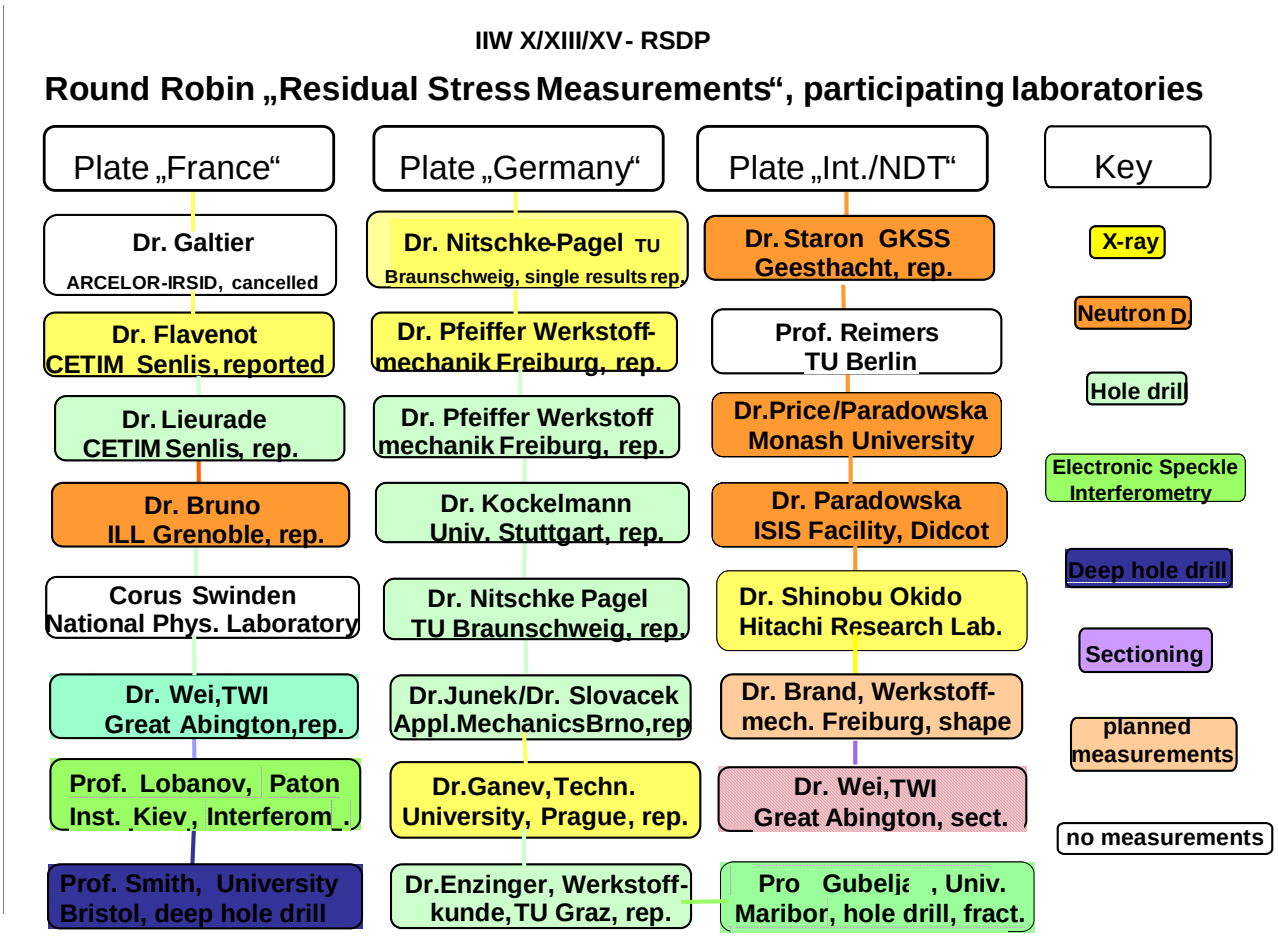

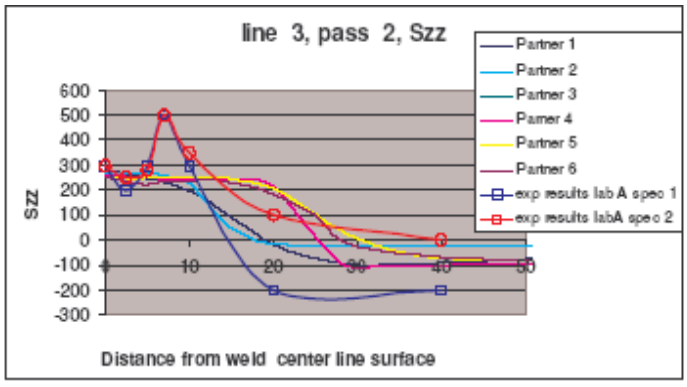

Fig.1 Calculated longitudinal residual stresses versus distance from the weld centre line in comparison with residual stress distributions measured by means of X-rays [1, 2]

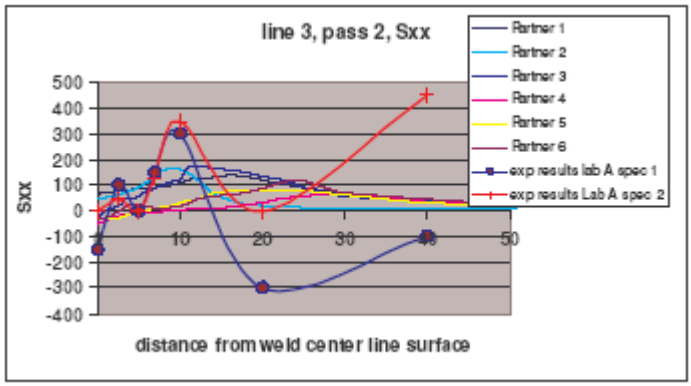

Fig.2 Calculated transverse residual stresses versus distance from the weld centre line in comparison with residual stress distributions measured by means of X-rays [1, 2]

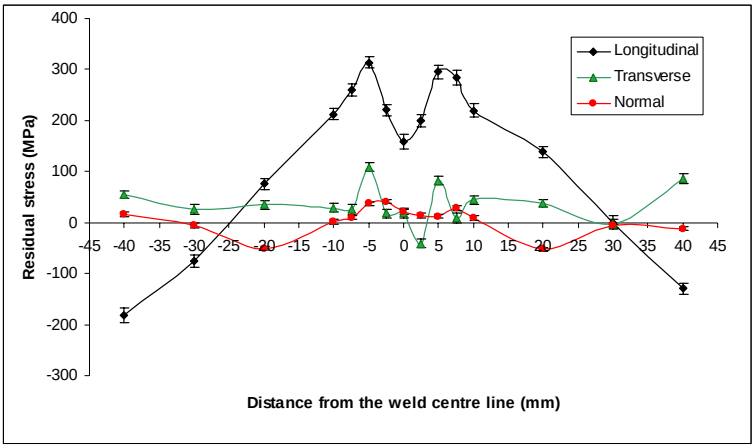

Fig. 3 Distribution of residual stresses versus distance from the weld centre line 3mm below the surface, neutron diffraction measurements, laboratory P, plate I [3]

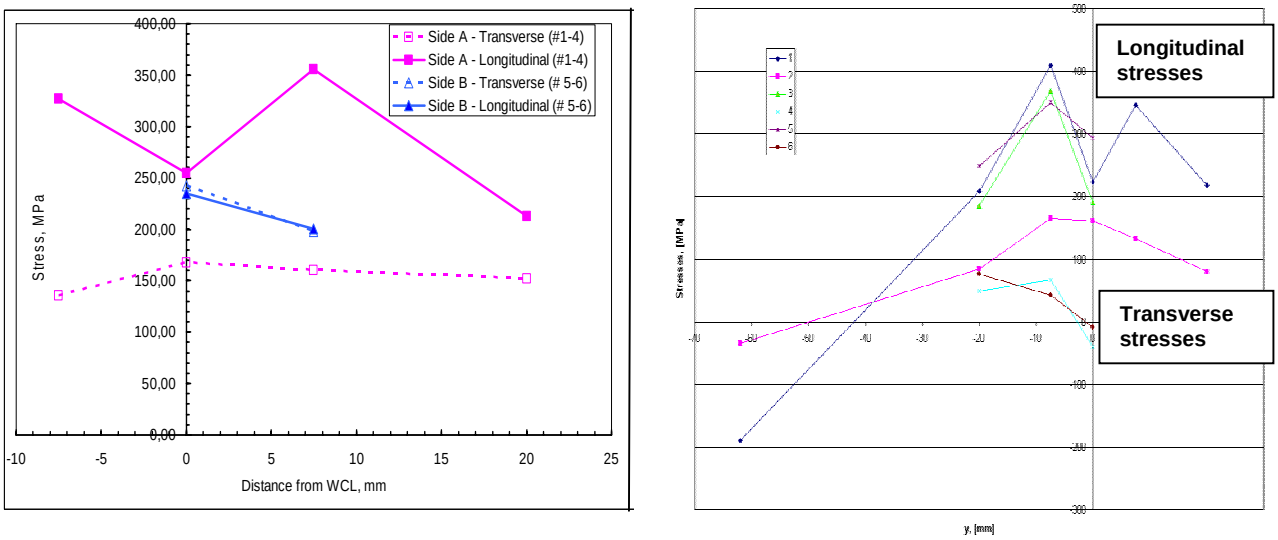

Fig.4 Distribution of residual stresses versus distance from weld centre line, measurements taken with hole drilling techniques. Left: stresses averaged over a thickness of 1.9 mm, laboratory K, plate III. Right: stresses averaged over a thickness of 1 mm, electron speckle-interferometry after hole drilling, laboratory M, plate III [3]

publication [4] reports for instance on smaller Bauschinger effects in a nitrogen-strengthened austenitic stainless steel if plastic straining is carried out at temperatures between 250 ^{0}C and 480 ^{0}C. Paper [5] mentions in a discussion on modelling that the hardening behaviour of an AISI 304-type austenitic stainless steel is a combination of isotropic hardening and kinematic hardening and that both hardening components are of the same order of magnitude.

According to these statements in literature and taking into account that temperatures in the HAZ of welded joints are even higher than 480 ^{0}C it seemed reasonable to check whether calculations with material laws like isotropic hardening or combinations of kinematic and isotropic hardening would offer a chance to solve the specific problem. In other words: whether the experimentally proven maxima of the longitudinal residual stresses could then also be revealed by calculations.

---

[3] IIW-Document IIW-XIII-2241-08, IIW-XV-1283-08: New results of the IIW Round Robin Residual Stress Measurements. Report on the Experimental Round Robin Tests on Residual Stresses 2008
[4] M.C. Matay, M.J. Carr, G. Krauss: The Bauschinger Effect in a Nitrogen-strengthened Austenitic Stainless Steel. Materials Science and Engineering 57 (1983) 205-222
[5] T. Manninen, P. Myllykoski, T. Taulavuori, A.S. Korhonen: Large-strain Bauschinger effect in austenitic stainless steel sheet. Materials Science and Engineering A 499 (2009) 333-336

This paper presents the results of new calculations of the residual stresses in the austenitic steel plate using pure isotropic strain hardening as well as different combinations of kinematic and isotropic strain hardening as materials law and in comparison also kinematic strain hardening and ideal elastic-plastic materials behaviour. A rather good agreement of the new calculations with measured results will be explained in terms of a pronounced strain hardening in the HAZ during welding and an overestimation of the Bauschinger effect with a kinematic hardening model.

The results of measurements of the angular distortion and of a bending round an axis transverse to the seam of the steel plate will also be reported and compared with calculations. These results are of interest for an explanation of the total distribution of residual stresses in the plate.

2. Calculations:

2.1 Conditions and parameters

The 3D calculations have been carried out with the finite element programme SYSWELD 2008. A mesh with about 55.000 linear volume elements of the type 3008 has been used. Fig. 5 presents the surface and a cross section of the used mesh. The elements in the top layers near the surface of the weld seam and the HAZ had a volume of 1mm³. The adding of filler material was modelled using the "chewing gum" method. The volume where the filler material should be added is modelled by elements wich are in an extremely soft material state. When the elements heat up over 1450°C the material state is changed to normal material with real material properties. The three bearing pins were idealised as an unmoveable constraint in depth direction and as soft springs in horizontal direction. The influence of the molten state of the filler material and of the basic material on the mechanical behaviour of the plate is considered by erasing the plastic strains and a reset of the stress-strain relation over 1450°C. The different examined and modelled hardening models are: isotropic hardening, kinematic hardening, combinations of both (25%, 50% and 75% isotropic hardening) and ideal elastic-plastic hardening behaviour.

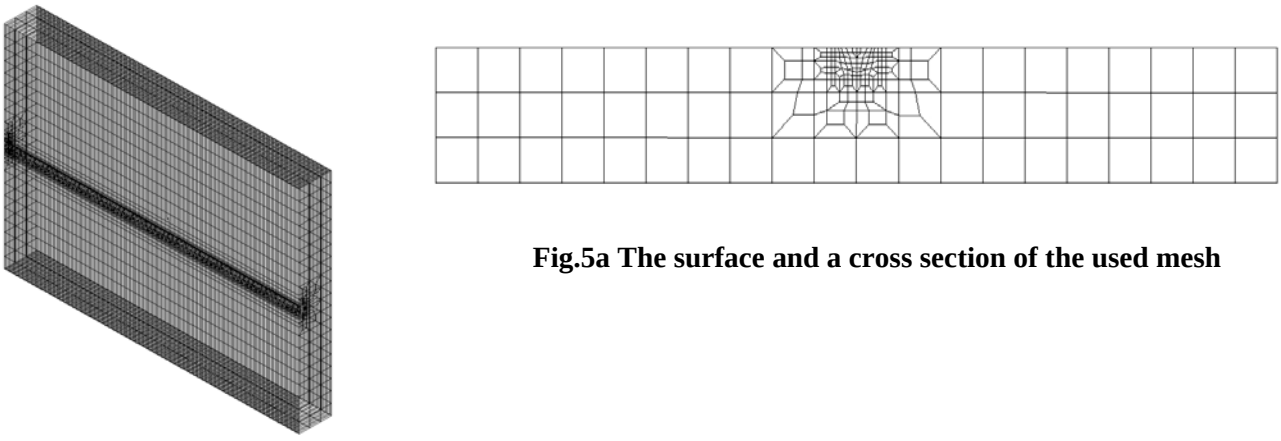

Fig.5a The surface and a cross section of the used mesh

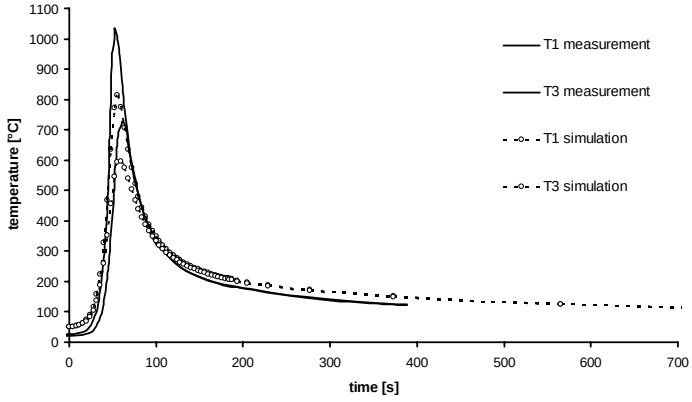

Fig 5b Comparison of the simulated and measured temperatures during the 2nd cycle

2.2 Results

2.2.1 3D calculations with a model with isotropic hardening as materials law

Fig. 6 to Fig. 8 present distributions of longitudinal residual stresses after the 2nd pass
- at the top side of the welded austenitic steel plate
- along a line at the top side perpendicular to the weld seam in a distance of 90 mm to the end of the plate
- over various cross sections of the plate-

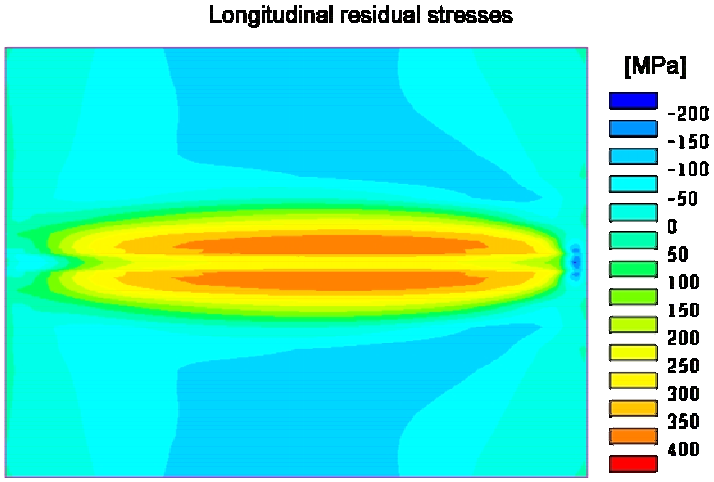

Fig. 6 Longitudinal residual stresses after the 2nd pass at the top side of the welded steel plate, 3D calculations with a model with isotropic hardening, 55 000 volume elements

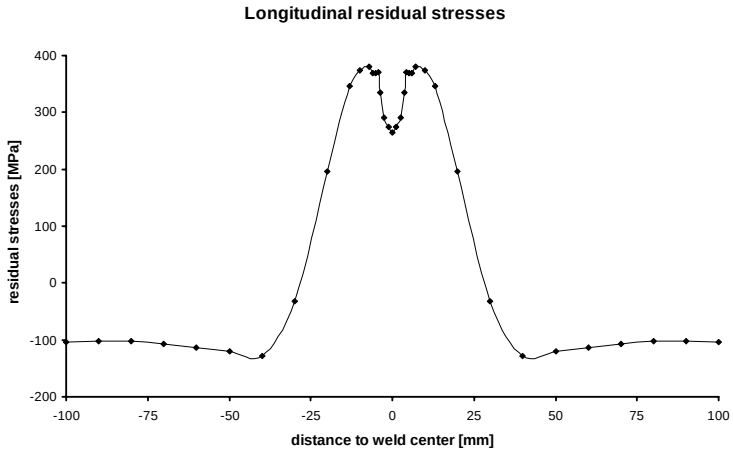

Fig. 7 Longitudinal residual stresses along a line perpendicular to the weld seam at the top side of the plate, distance to the end of the plate 90 mm

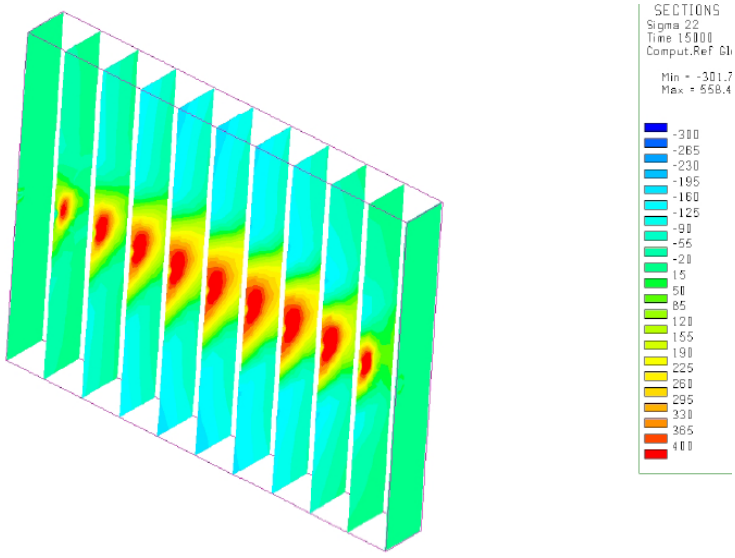

Fig. 8 Longitudinal residual stresses over various cross sections of the plate

All figures demonstrate a relative minimum of the residual stress magnitudes (≈270 MPa) at the weld centre line and maxima (≈380 MPa) on both sides of the weld seam in a distance of 7 mm from the centre line. The distribution of residual stresses over various cross sections indicates high tensile stresses with magnitudes up to ≈550 MPa below the surface layers and decreasing magnitudes of tensile stresses in bigger distances from the surface.

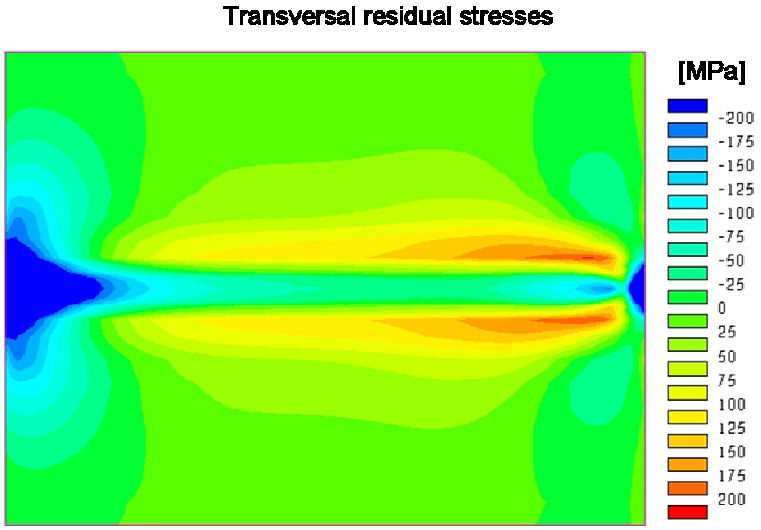

Fig. 9 Transverse residual stresses after the 2nd pass at the top side of the welded steel plate, 3D calculations with a model with isotropic hardening, 55 000 volume elements

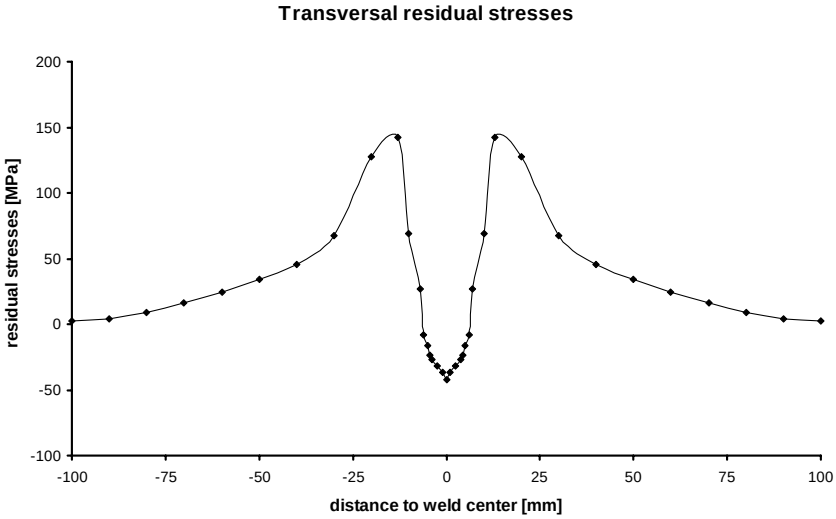

Fig.10 Transverse residual stresses along a line perpendicular to the weld seam at the top side of the plate, distance to the end of the plate 90 mm

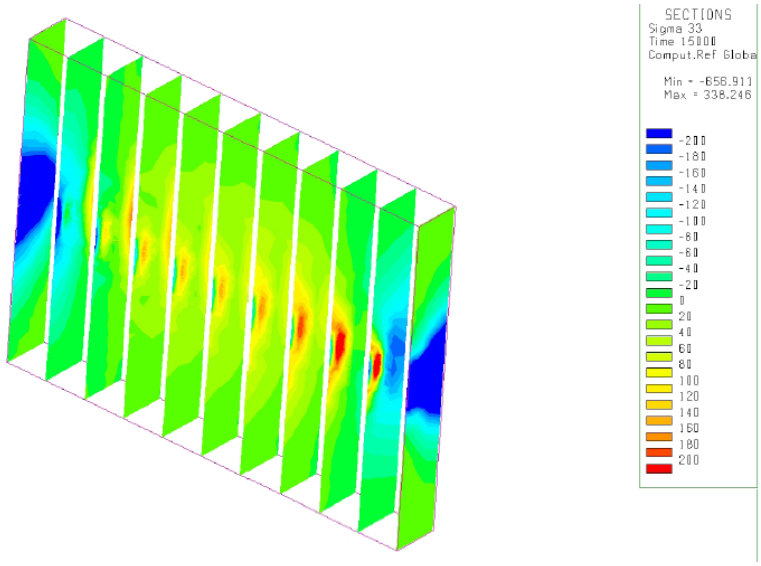

Fig. 11 Transverse residual stresses over various cross sections of the plate

Fig. 9 to Fig.11 exhibit distributions of transverse residual stresses after the 2nd pass, again

- at the top side of the welded austenitic steel plate
- along a line perpendicular to the weld seam at the top side in a distance of 90 mm to the end of the plate
- across various cross sections of the plate

Fig. 9 indicates that the distribution of transverse residual stresses is not symmetric with respect to a middle line transverse to the weld seam. The maxima of the tensile stresses are closer to one end of the seam. The distribution of the residual stresses along a line transverse to the seam in a distance of 90 mm from the end of the plate (Fig. 10) indicates tensile maxima of nearly 150 MPa in a distance of ca. 10 mm from the weld centre line and a stress minimum of nearly -50 MPa at the centre line. Fig. 11 reveals significant tensile residual stresses below the centre line of the seam.

2.2.2 3D calculations with models with kinematic hardening

For comparison and for clearness the results of calculations with models with kinematic hardening respectively a mixture of 25% kinematic hardening and 75 % isotropic hardening are also shown. Fig. 12 and Fig. 13 illustrate the results for longitudinal respectively transverse residual stresses in comparison with the results of calculations with pure isotropic hardening. The figures indicate that a mixture of 25% kinematic and 75% isotropic hardening lowers the maximum tensile values of the longitudinal as well as of the transverse residual stresses. The minimum compressive magnitudes of the transverse stresses at the weld centre line are also reduced a little bit. Contrasting to these results calculations with a pure kinematic hardening model demonstrate no tensile maxima of the longitudinal residual stresses in the HAZ (Fig. 12) but lower magnitudes of the longitudinal residual stresses in the range of the yield strength of the material (275 MPa) and a small maximum at the weld centre line. The minimum of transverse residual stresses at the weld centre line is also reduced in comparison with the calculated results using isotropic hardening models. This minimum reaches only very small magnitudes in the compressive range.

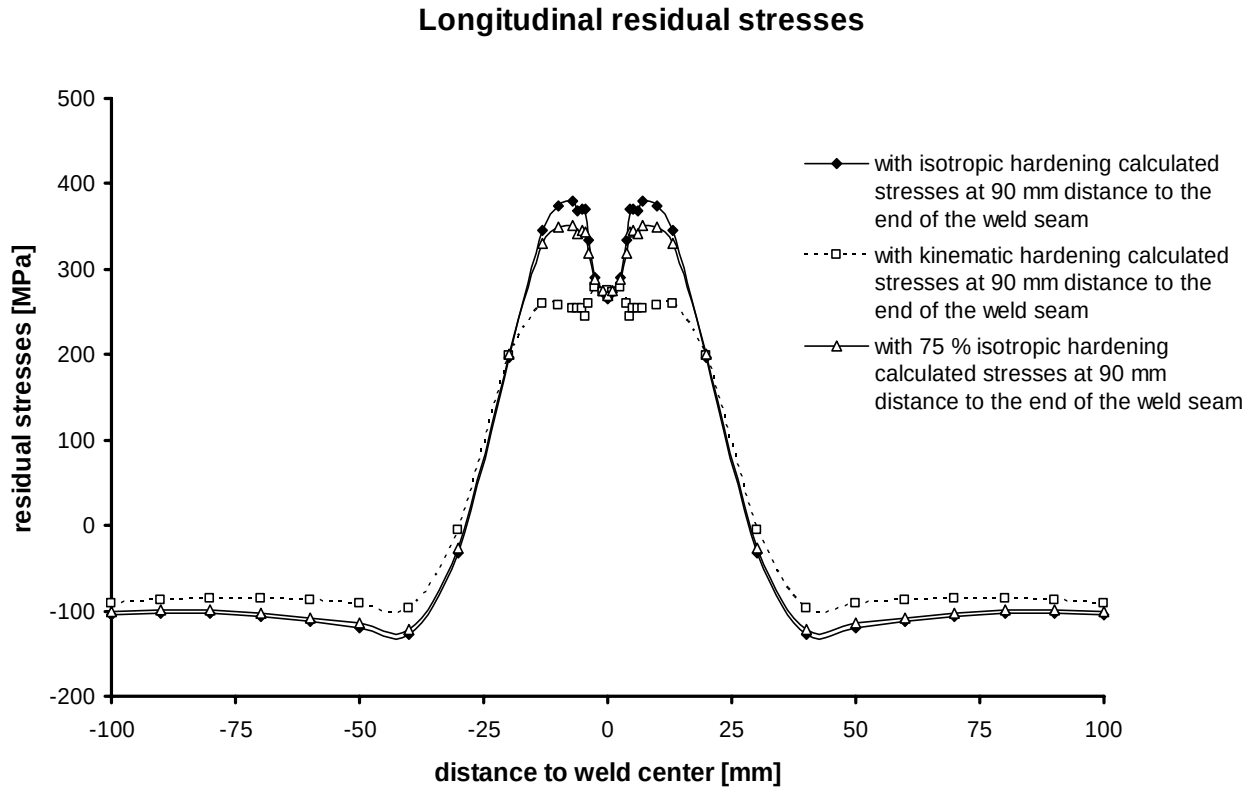

Fig. 12 Comparison of calculations of the longitudinal residual stresses using different material laws

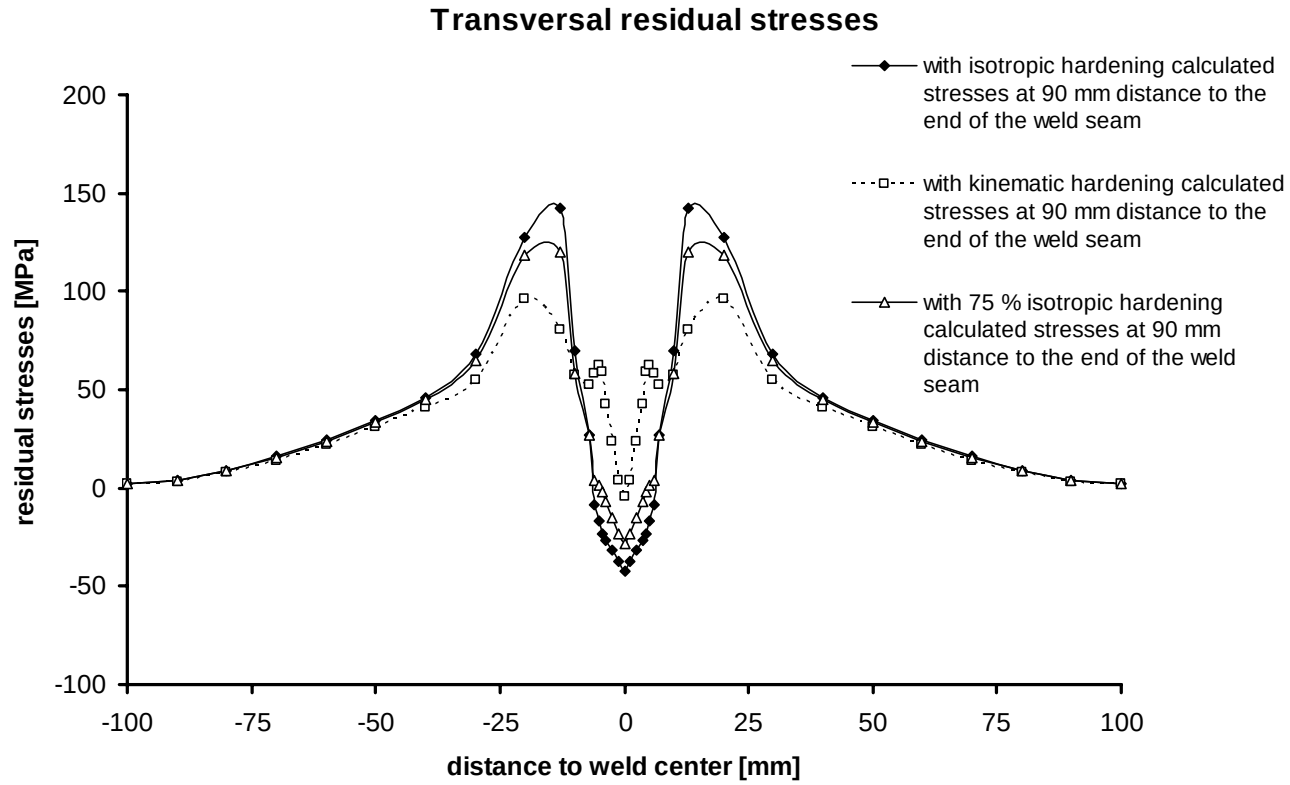

Fig. 13 Comparison of calculations of the transverse residual stresses using different material laws

3. Comparison between calculated and measured residual stress distributions

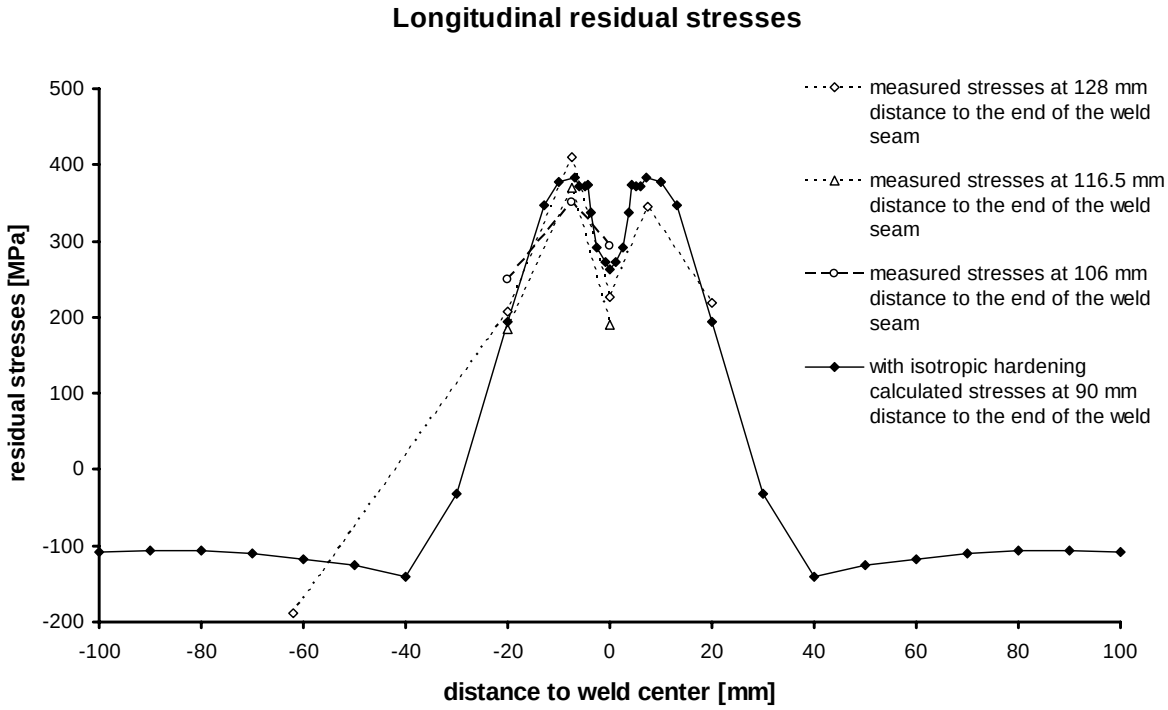

Fig. 14 Longitudinal residual stresses measured by means of the hole drilling method in combination with electron speckle-inter-ferometry in different distances to the end of the seam, comparison with calculated residual stresses using the model of isotropic hardening

All measurements presented in the first chapter (Fig. 3 and Fig.4) demonstrate tensile maxima of the longitudinal stresses in the HAZ in distances between 5 mm and 8 mm from the weld centre line. It is evident that the magnitudes of these maxima depend upon the depth of the surface layer over which each measuring method is integrating the residual stresses. The highest peak values have been found by means of X-rays (≈ 500 MPa, measuring depth ≈ 10μm, [3]), followed by hole drilling methods with a measuring depth of 1.9mm and 1.0 mm (≈350 MPa – ≈400 MPa) and by neutron diffraction (≈300MPa). It seams reasonable therefore to compare the calculated results especially with the results measured by the hole drilling method in combination with electron speckle interferometry which is integrating the stresses exactly over the same depth as the calculations do, that is 1mm. Fig. 14 and Fig. 15 present such comparisons for the longitudinal and the compressive residual stresses.

In Fig 14 a rather good agreement of the calculated stresses with the measured ones is evident. With one exception the measured peak stresses are a little bit lower than the calculated ones. The measured minimum tensile stresses at the weld centre line are, with one exception, also somewhat lower than the calculated ones. The measured minimal tensile stresses go down to ≈200 MPa, whereas the calculated ones remain at the value of the yield strength of the material (≈270 MPa).

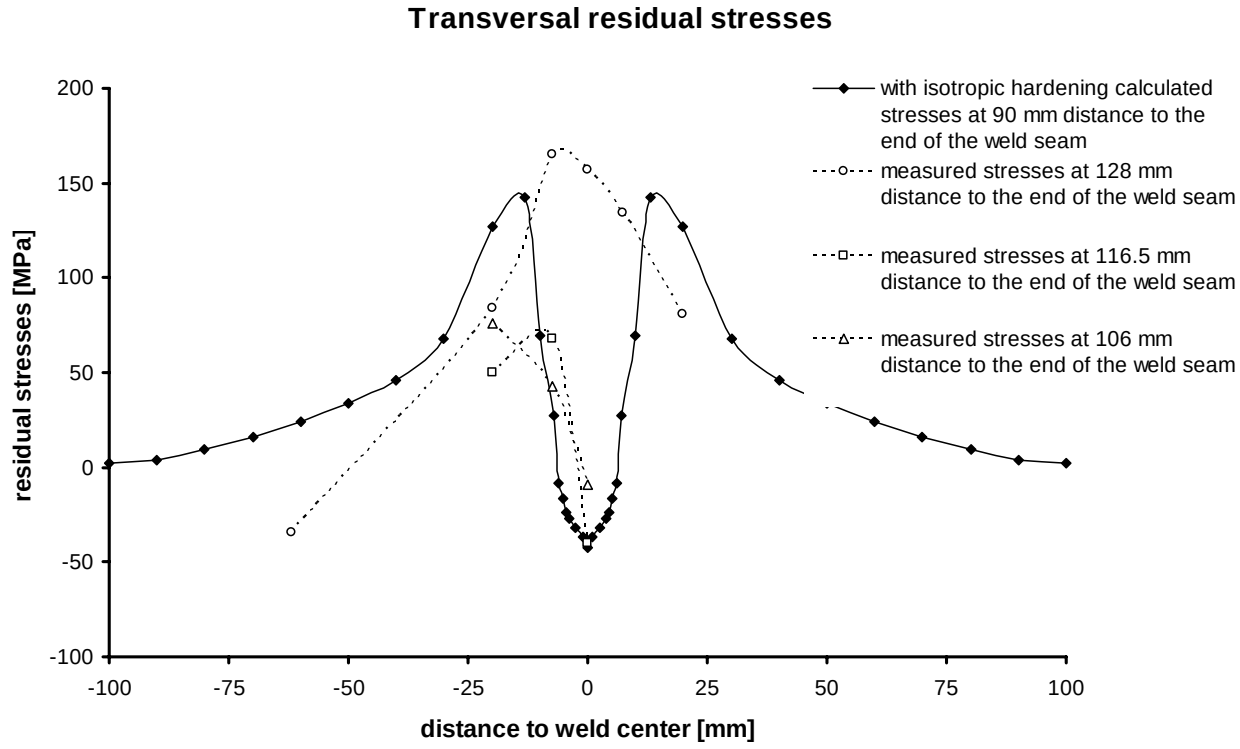

Fig. 15 Transverse residual stresses measured by means of the hole drilling method in combination with electron speckle-interferometry in different distances to the end of the seam, comparison with calculated residual stresses using the model of isotropic hardening

The situation for the transverse residual stresses is not as clear as for the longitudinal stresses. Measurements by means of X-rays indicate pronounced tensile stress maxima (≈300 MPa) in a distance of ≈10 mm from the weld centre line and a minimum of the residual stresses in the compressive range at the weld centre line [3]. Neutron diffraction reveals tensile stress maxima of ≈100 MPa and a stress minimum at he weld centre line in the compressive range (Fig. 3). But from the results of the hole drilling method in combination with electron speckle-interferometry only two measurements indicate stress minima at the weld centre line in the compressive range and are

in a rather good agreement with the calculated stresses (Fig. 15). The measurement in a distance of 128 mm from the end of the weld seam shows clearly a tensile stress maximum of more than 150 MPa at the weld centre line. This extraordinary result is obviously in contradiction with the calculated results. Whether this discrepancy could be explained by the asymmetric distribution of the transverse residual stresses shown in Fig. 9 is not clear at the moment.

4. Measurements of distortions

Distortions have been measured with a displacement transducer on a CNC machine tool [6]. The accuracy of measurements was 1/1000mm. Fig. 16 to 18 illustrate the measured distortions in comparison with different calculations. As can be seen in Fig. 16 and 17 the bending round an axis transverse to the seam is much less pronounced - nearly negligible – in comparison with the angular distortion. The differences between the measured and the calculated values are rather small. Details of the calculations with somewhat different programs are still under discussion (Fig. 17 and Fig.18).

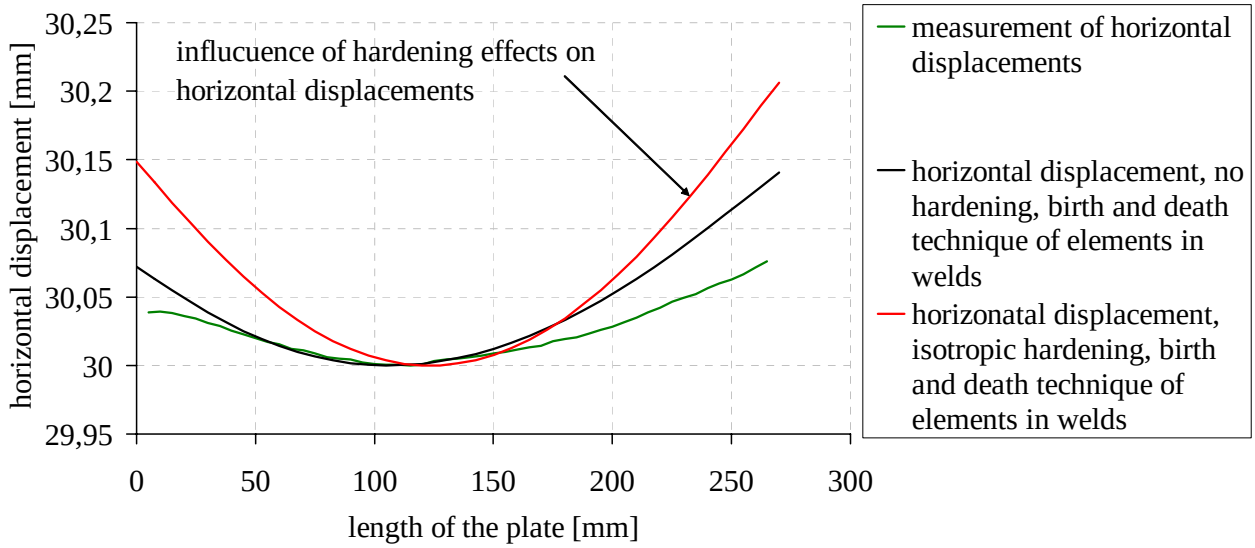

Fig 16 Measured and calculated values of bending round an axis transverse to the weld seam (Brand)

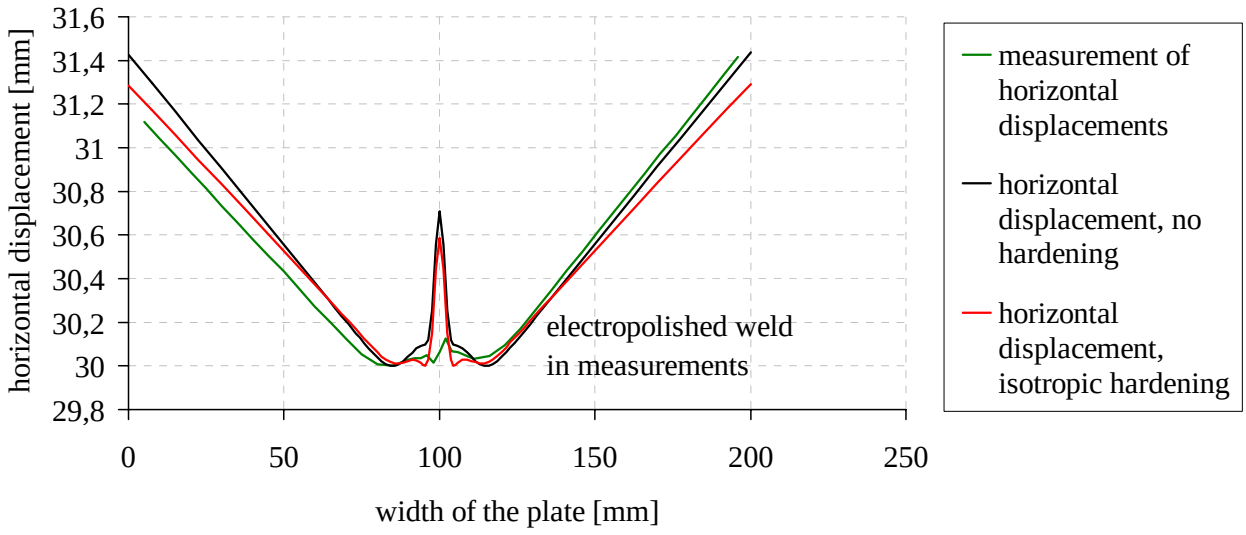

Fig. 17 Measured and calculated values of angular distortion (Brand)

[6] Manufacturer Deckel MAHO, DMU 50T

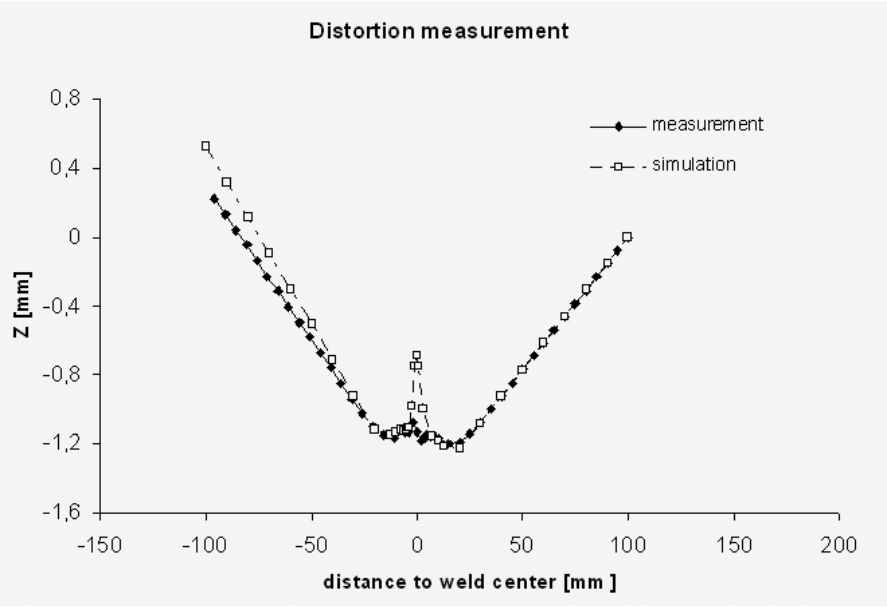

Fig. 18 Measured (Brand) and calculated values of angular distortion, calculations with isotropic hardening

5. Discussion

The model consideration in Fig 19 explains that in the isotropic hardening model the flow stress after a load reversal will not be changed, but remains constant at the value reached at the end of the first load cycle. On the other side, the kinematic hardening model takes into account the Bauschinger effect, that is to say the beginning of plastic flow after the load reversal is lowered compared with the onset of plastic flow during the first load cycle. According to the model in Fig. 19 [7[1]] the beginning of plastic flow in the second load cycle is $\sigma = \sigma_1 - 2\sigma_0$, if σ_1 is the load stress at the beginning of the load reversal and σ_0 is the original yield stress of the material. But the model diagram demonstrates also that the hardening behaviour of real materials may not strictly obey the kinematic hardening rule, but is between the kinematic and the isotropic hardening behaviour. Therefore in cold forming the Bauschinger effect has to be taken into account fully or partially with a hardening law appropriate to the specified material. That could be a mixed hardening model with specific amounts of isotropic and kinematic hardening, as for instance reported in [5].

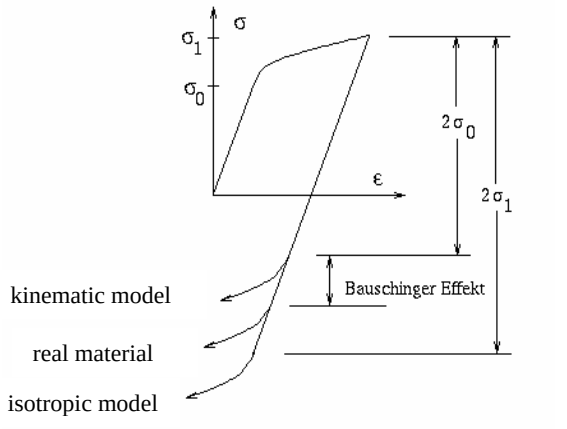

Fig.19 Model consideration in order to explain the difference of kinematic and isotropic hardening. During welding the sequence of the first and the second load cycle starts in the opposite direction of the figure: 1st cycle heating with increasing compressive stresses in the HAZ, 2nd cycle cooling down with increasing tensile stresses in the HAZ

On the other side paper [4] reports that the efficiency of the Bauschinger effect will be reduced, if the material is heated during cycles of plastic deformation, for instance up to 480 ^{0}C. In welding much higher temperatures are reached during the first load cycle, which is the expansion of the

[7] Dr. Lothar Schreiber: Vorlesung Plastizitätstheorie 2, Technische Universität Kassel

base material due to heating up. Actually it is not known whether the Bauschinger effect will be even more reduced in connection with higher deformation temperatures than 480 ^{0}C. But it seams reasonable to compare the consequences of an effective or an absent Bauschinger effect for the development of residual stresses.

In any case during the first load cycle, the heating up, the thermal expansion in the area close to the weld seam will induce compressive stresses. As these increasing stresses reach the decreasing yield strength the material close to the weld seam will be plastically deformed in connection with a work hardening effect. With values calculated by the kinematic as well as by the isotropic hardening model Fig 20 offers an information about the amount of accumulated plastic strain near the weld seam.

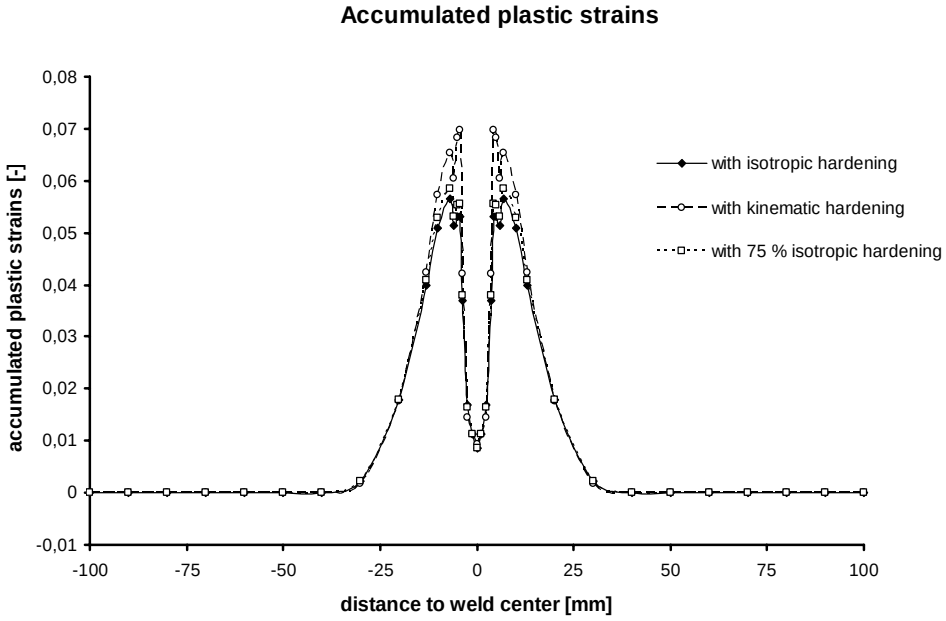

Fig. 20 Accumulated plastic strain calculated with isotropic, kinematic and mixed hardening

During cooling down of the material in the second load cycle tensile stresses will develop in the HAZ and will increase with decreasing temperature. These increasing tensile stresses can be limited finally by the yield strength calculated for the second cycle after load reversal with the used hardening law – either kinematic or isotropic hardening.

If the kinematic hardening model is used, as described in Fig. 19, rather low yield strength values will be calculated for this second load cycle. Consequently the resulting tensile residual stresses must be limited to these yield strength values in the HAZ. The results of all calculations using the kinematic hardening law seam to indicate such a case: namely nearly constant tensile residual stresses with amounts in the range of the yield strength at room temperature.

If the isotropic hardening model is used for calculations the consequences of a - for instance remarkable – work hardening during heating of the HAZ can become fully effective. Increased yield strength values can be anticipated during cooling down and finally at room temperature in the hardened area close to the weld seam. Consequently the developing tensile stresses are limited only by these enhanced yield strength values and can become higher than with the kinematic hardening model. That is how a maximum of the tensile residual stresses in the longitudinal direction is understandable. Interesting enough Fig. 20 presents maxima of the accumulated plastic strain of ca. 5.7 % in the HAZ and table 2 with all work hardening values of the material indicates a yield strength of 419 MPa at room temperature after a plastic strain of 5%. Therefore magnitudes of nearly 400 MPa of the maximum tensile stresses seam really possible.

The comparison of the distributions of transverse residual stresses computed by using the kinematic hardening model or the isotropic hardening model does not show fundamental qualitative discrepancies, but noticeable quantitative discrepancies. The maxima of the tensile

Work hardening

Temperature (°C)	20	100	200	300	400	500	600	700
Strain (%)	Stress (MPa)							
0.2	275	238	198	172	157	151	145	136
1	314	263	231	200	187	179	170	160
5	419	359	334	307	294	282	262	211
20	561	490	470	451	435	419	387	340

Temperature (°C)	800	900	1000	1100	1200	1300	1400
Strain (%)	Stress (MPa)						
0.2	127	115	78	38	24	16	2
1	151	137	82	38	24	22	2
5	198	161	96	39	25	22	2
20	293	169	100	44	29	23	2

Table 2 Work hardening of the investigated material 316LNSPH at different temperatures and different strains

residual stresses are ca. 150 MPa with the isotropic hardening model respectively ca. 100 MPa with the kinematic hardening model and the minimum residual stresses at the weld centre line are ≈-50MP a respectively ≈-20MPa (Fig.13). The comparison with measured transverse residual stresses (Fig. 3, Fig.4, Fig. 15) reveals a principle agreement of the calculated and measured distributions of the transverse residual stresses, but cannot really prove the validity of the calculations with the isotropic hardening model. It may be mentioned that the small secondary maxima of ca. 60MPa in the distribution of the transverse stresses calculated with the kinematic hardening model (Fig. 13) have also be found in the results measured by means of X-rays [3].

6. Concluding remark

The new results reveal that at least for austenitic stainless steels of the type 316L calculations with the isotropic hardening model are in a rather good agreement with measured residual stress distributions. Especially the maxima of the longitudinal residual stresses in the HAZ on both sides of the weld seam can be reproduced, whereas calculations with the kinematic hardening model indicated only rather flat distributions with relatively low magnitudes (270 MPa) across the weld seam and in a part of the HAZ. Therefore, one can conclude that the Bauschinger effect has not to be taken into account for calculations of residual stresses due to welding of such steels. Further investigations should be carried out in order to clarify whether the Bauschinger effect is of any significance for residual stresses due to welding of other steel types or whether the heating to high temperatures removes the efficiency of it and calculations could be done by using the isotropic hardening model.

Acknowledgement

The coordinator would like to thank for all contributions to this document.